High-Sensitivity Atomic Magnetometer Unaffected by Spin-Exchange Relaxation

J. C. Allred and R. N. Lyman
Department of Physics, Univerisity of Washington, Seattle, Washington 98195

T. W. Kornack and M. V. Romalis*
Department of Physics, Princeton University, Princeton, New Jersey 08544
(Received 6 March 2002; published 9 September 2002)

Alkali-metal magnetometers compete with SQUID detectors as the most sensitive magnetic field sensors. Their sensitivity is limited by relaxation due to spin-exchange collisions. We demonstrate a K magnetometer in which spin-exchange relaxation is completely eliminated by operating at high K density and low magnetic field. Direct measurements of the signal-to-noise ratio give a magnetometer sensitivity of 10 fT $\mathrm{Hz}^{-1/2}$, limited by magnetic noise produced by Johnson currents in the magnetic shields. We extend a previous theoretical analysis of spin exchange in low magnetic fields to arbitrary spin polarizations and estimate the shot-noise limit of the magnetometer to be 2×10^{-18} T $\mathrm{Hz}^{-1/2}$.

DOI: 10.1103/PhysRevLett.89.130801 PACS numbers: 07.55.Ge, 32.80.Bx, 33.35.+r

Sensitive magnetometers find a wide range of applications, from tests of fundamental symmetries to measurements of biological magnetic fields. Low temperature SQUID detectors presently hold the record as the most sensitive magnetometers with a noise level of about 1 fT $\mathrm{Hz}^{-1/2}$. Alkali-metal magnetometers using K [1] and Rb [2,3] atoms approach this level of sensitivity. Their fundamental sensitivity limit is due to shot-noise,

$$\delta B = \frac{1}{\gamma \sqrt{n T_2 V t}}, \tag{1}$$

where n is the density of atoms, γ is their gyromagnetic ratio, T_2 is the transverse spin relaxation time, V is the cell volume, and t is the measurement time. Spin-exchange collisions often limit the relaxation time $T_2^{-1} \sim T_{\mathrm{SE}}^{-1} = n \bar{v} \sigma_{\mathrm{se}}$, where $\bar{v}$ is the thermal velocity and $\sigma_{\mathrm{se}} \simeq 2 \times 10^{-14}$ cm^2 is the spin-exchange cross section. This process limits the sensitivity of alkali-metal magnetometers to about 1 fT $\mathrm{cm}^{3/2}$ $\mathrm{Hz}^{-1/2}$. For example, the sensitivity of the Rb magnetometer in [3] is estimated to be 0.3 fT $\mathrm{Hz}^{-1/2}$ for a 500 cm^3 cell.

In this Letter, we describe an alkali-metal magnetometer that completely eliminates spin exchange as a source of relaxation. We obtain a resonance linewidth of 1.1 Hz for K atoms at a density of $n = 10^{14}$ cm^{-3}, where the spin-exchange rate is 1.2×10^5 sec^{-1}. For high K density the shot-noise sensitivity is limited by the K-K spin-destruction cross section $\sigma_{\mathrm{K}}^{\mathrm{SD}} = 1 \times 10^{-18}$ cm^2 [4]. Thus, magnetic field sensitivities on the order of 10^{-17} T $\mathrm{cm}^{3/2}$ $\mathrm{Hz}^{-1/2}$ can be achieved.

Spin-exchange collisions usually contribute to transverse spin relaxation even though they preserve the total angular momentum projection $m_{F_1} + m_{F_2}$ of the colliding atoms. In a magnetic field the expectation values $\langle m \rangle_F$ in the two hyperfine states precess in opposite directions

$$\omega_{F=I\pm 1/2} = \pm \frac{g_s \mu_B B}{(2I+1)\hbar}, \tag{2}$$

and spin-exchange collisions contribute to relaxation of transverse coherences by changing the F quantum number. However, in very small magnetic fields, such that $\omega T_{\mathrm{SE}} \ll 1$, the expectation values $\langle m \rangle_F$ in the two hyperfine states become locked together by rapid spin exchange and precess in the same direction [5]. For small atomic polarization the spin precession rate is given by

$$\omega_0 = \frac{g_s \mu_B B}{q \hbar}, \quad \text{where} \quad q = \frac{S(S+1) + I(I+1)}{S(S+1)} \tag{3}$$

is the slowing-down factor due to nuclear angular momentum [6]. In this limit spin exchange contributes to transverse relaxation only in second order and vanishes for zero magnetic field [7],

$$\frac{1}{T_2^{\mathrm{SE}}} = \omega_0^2 T_{\mathrm{SE}} \left[\frac{1}{2} - \frac{(2I+1)^2}{2q^2} \right] q^2. \tag{4}$$

In the absence of spin-exchange relaxation spin-destruction collisions due to the spin-rotation interaction [8] become a limiting factor. We use a combination of K and He atoms in our magnetometer because they have small spin-destruction cross sections for alkali-alkali and alkali-buffer gas collisions, as shown in Table I. He buffer gas is added to slow down diffusion of K atoms to cell walls.

We use the zero-field pump-probe arrangement [14] shown in Fig. 1. K atoms are contained in a 2.5 cm diam spherical cell made from GE180 aluminosilicate glass. The cell is filled with several atm of ^{4}He and 30 torr of N_2 gas necessary for quenching of K atoms. It is placed in an oven constructed from high-temperature plastic materials and heated to 190 °C by flowing hot air. We use a set of five nested cylindrical magnetic shields

TABLE I. Alkali-metal spin-destruction cross sections.

Alkali metal	σ^{SD}_{Self}	σ^{SD}_{He}	σ^{SD}_{Ne}	$\sigma^{SD}_{N_2}$
K	1×10^{-18} cm^2 [4]	8×10^{-25} cm^2 [9,10]	1×10^{-23} cm^2 [10]	
Rb	9×10^{-18} cm^2 [9]	9×10^{-24} cm^2 [9]		1×10^{-22} cm^2 [11]
Cs	2×10^{-16} cm^2 [12]	3×10^{-23} cm^2 [13]		6×10^{-22} cm^2 [13]

with a shielding factor of 10^6. The diameter of the inner shield is 16'' and we minimize the amount of conductive materials within the shield to reduce noise from Johnson currents. A set of coils inside the shields allows control of all three components of the magnetic field. K atoms are optically pumped by a 1 W multimode diode laser. A single mode diode laser probes the polarization of the atoms. The $\hat{x}$ component of the K spin polarization is measured using either optical rotation of off-resonant light or circular dichroism of the vapor. Both methods give similar performance in our conditions.

Since the transverse spin relaxation time is one of the fundamental parameters determining the shot-noise limit, we measure it directly using a synchronous pumping technique. A magnetic field of 50–200 μG is applied in the $\hat{y}$ direction and the pumping beam is chopped at a frequency close to the resonance condition given by Eq. (3). The precession of the polarization around the magnetic field is detected using the probe beam. A resonance curve obtained using this technique is shown in Fig. 2. The resonance is well described by a simple Lorentzian with the half-width given by $\Delta\nu = (2\pi q T_2)^{-1}$. Care is taken to operate well in the regime of low pump and probe intensity. From the fit to the data we obtain $T_2 = 22$ ms for $[\mathrm{K}] = 10^{14}$ cm^{-3} and $[\mathrm{He}] = 6 \times 10^{19}$ cm^{-3}. Excluding the contribution of spin exchange, T_2 is given by

$$\frac{1}{T_2} = \frac{1}{T_D} + \sigma^{SD}_{He}\bar{v}[\mathrm{He}] + \sigma^{SD}_{K}\bar{v}[\mathrm{K}] + \sigma^{SD}_{N_2}\bar{v}[\mathrm{N_2}], \quad (5)$$

where σ^{SD} are the spin-destruction cross sections and T_D is the relaxation time due to diffusion, approximately given by Eq. (11). Using cross sections listed in Table I and K-He diffusion constant from [10] we estimate $T_2 = 30$ ms with approximately equal contributions from diffusion, K-K, and K-He collisions. This value is in good agreement with the experimentally measured width given the uncertainties in the spin-destruction cross sections. At higher magnetic fields the resonance width increases due to the second-order contribution of spin exchange [7]. Figure 3 shows this dependence together with a fit based on Eq. (4). From the fit we obtain $T_{SE} = 7.6\,\mu$s, in good agreement with existing measurements of the spin-exchange cross section [15,16].

The magnetometer can be operated in several modes to measure different components of the magnetic field. Here we focus on the operation with all three components of the magnetic field close to zero relative to the bandwidth. In this mode the magnetometer is sensitive only to the B_y field, which tilts the polarization into the $\hat{x}$ direction. Also, the light shifts due to both the pump and the probe beams are suppressed by two small factors and the resonance is not broadened by variation of the gyromagnetic

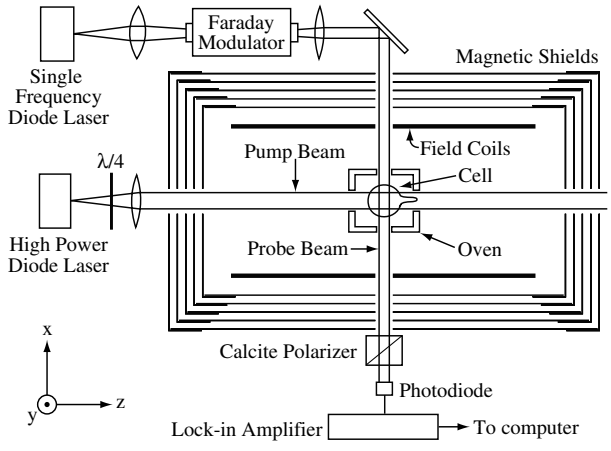

FIG. 1. Experimental implementation of the K magnetometer. Transverse polarization is detected using optical rotation.

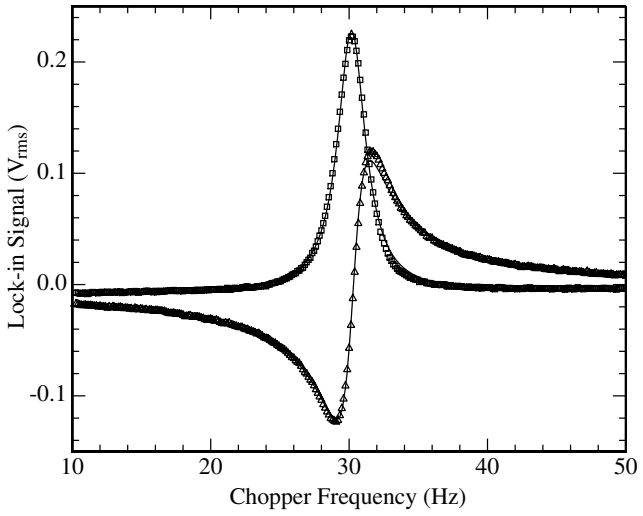

FIG. 2. Transverse resonance of the magnetometer. Both the inphase (squares) and out-of-phase (triangles) signals are shown. The fit is a Lorentzian with a half-width of 1.2 Hz.

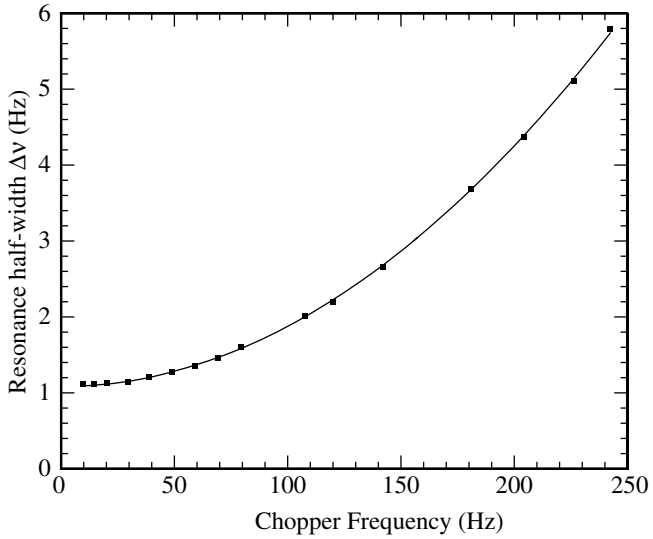

FIG. 3. Spin-exchange broadening of the resonance linewidth. The fit based on Eq. (4) gives $T_{\mathrm{SE}} = 7.6\,\mu$s and a limiting low-frequency linewidth of 1.1 Hz

ratio with polarization [see Eq. (9)]. To measure the magnetic noise of the magnetometer we apply a small sinusoidal modulation to the B_y field and record the frequency spectrum of the magnetometer response. A series of such frequency spectra are shown in Fig. 4. For this data the bandwidth of the magnetometer was increased to 10 Hz by using a higher pumping rate. From the signal-to-noise ratio we determine the noise level of the magnetometer to be 10 $\mathrm{fT_{rms}\,Hz^{-1/2}}$ independent of frequency.

This noise level is dominated by the magnetic fields produced by thermal Johnson currents flowing in the

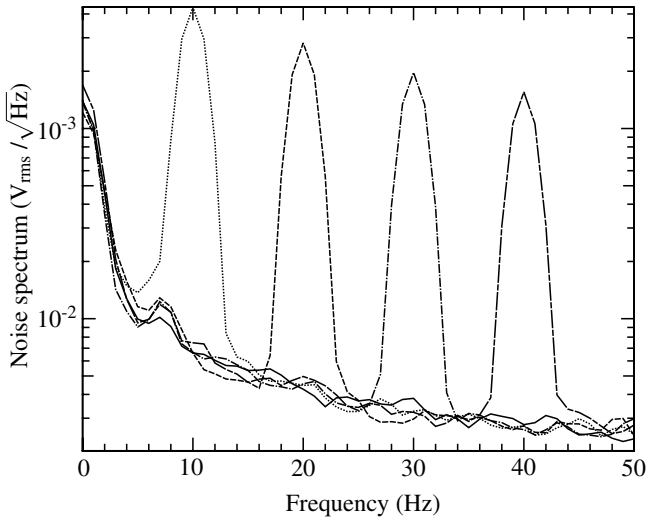

FIG. 4. Magnetometer spectra with a 700 $\mathrm{fT_{rms}}$ modulation of B_y field at 10, 20, 30, and 40 Hz (solid and dashed lines). S/N = 70 ± 10 at all frequencies as expected for Johnson noise.

magnetic shields [17,18]. We use the equations given in [19] for magnetic noise from a high-permeability infinite slab to estimate the noise for our cylindrical shields to be $7 \pm 2\ \mathrm{fT\,Hz^{-1/2}}$ independent of frequency up to about 200 Hz. Thus, Johnson noise limits the magnetic field sensitivity that can be obtained using conventional magnetic shields. In contrast, SQUID detectors are usually tested in superconducting shields.

To obtain an accurate estimate of the shot-noise sensitivity of the magnetometer and characterize its other properties we extend the analysis in [5,7] allowing for an arbitrary degree of spin polarization. For high buffer gas pressures the hyperfine structure is not resolved and the evolution of the density matrix ρ is well described by [6]

$$\frac{d\rho}{dt} = D\nabla^2\rho + \frac{[H,\rho]}{i\hbar} + \frac{\varphi(1 + 4\langle\mathbf{S}\rangle\cdot\mathbf{S}) - \rho}{T_{\mathrm{SE}}} + \frac{\varphi - \rho}{T_{\mathrm{SD}}} + R[\varphi(1 + 2\mathbf{s}\cdot\mathbf{S}) - \rho], \tag{6}$$

where $\varphi = \rho/4 + \mathbf{S}\cdot\rho\mathbf{S}$ is the purely nuclear part of the density matrix and $H = A\mathbf{I}\cdot\mathbf{S} + g_s\mu_B\mathbf{B}\cdot\mathbf{S}$ [20]. Here R is the optical pumping rate, T_{SD} is the relaxation time due to spin-destruction collisions, and $\mathbf{s}$ is the optical pumping vector, giving the direction and the degree of circular polarization of the light. We first neglect the diffusion term and note that for a magnetic field $\mathbf{B}$ parallel to the direction of optical pumping $\mathbf{s}$ (or equal to zero), the density matrix is described by a spin-temperature distribution $\rho_{ST} \propto e^{m_F\beta}$ with the electron spin polarization $P = \tanh(\beta/2) = sR/(R + T_{\mathrm{SD}}^{-1})$ [6]. To find a steady-state solution for an arbitrary magnetic field we write $\rho = \varphi\exp(\boldsymbol{\beta}\cdot\mathbf{S})/2\cosh(\beta/2)$ and obtain an equation for the purely electronic part of the density matrix. For a magnetic field in the $\hat{y}$ direction and optical pumping in the $\hat{z}$ direction we obtain

$$P_x = \frac{g_s\mu_B B_y}{\hbar}\frac{sR}{(g_s\mu_B B_y/\hbar)^2 + (R + T_{SD}^{-1})^2} \tag{7}$$

$$P_z = \frac{sR(R + T_{SD}^{-1})}{(g_s\mu_B B_y/\hbar)^2 + (R + T_{SD}^{-1})^2}. \tag{8}$$

Note that the steady-state response of the polarization does not depend on the alkali-metal nuclear spin.

Other results are obtained by considering the time evolution of the density matrix. We solve Eq. (6) analytically by writing $\rho = \rho_{\mathrm{ST}} + \tilde{\rho}$, where $\tilde{\rho}$ is a small deviation from the spin-temperature distribution such that $\mathrm{Tr}(\tilde{\rho}\mathbf{S}) = 0$. We perform all calculations to first order in $\tilde{\rho}$, which is suppressed by the ratio of the spin-exchange rate to other relevant rates. We find that the atoms precess around the B_y field at a rate that depends on the degree of their polarization. For K atoms ($I = 3/2$) we obtain

$$\omega = \frac{g_s\mu_B B}{\hbar}\frac{\cosh(\beta)}{2 + 4\cosh(\beta)}. \tag{9}$$

For small β this expression is in agreement with Eq. (3) while for large β the precession rate approaches the value given by Eq. (2) since most atoms occupy $F = 2, m = 2$ state and are not affected by spin exchange. We also find that the frequency response of the magnetometer is equivalent to a first order low-pass filter with a cutoff frequency

$$f_c = \frac{(R + T_{\mathrm{SD}}^{-1})}{2\pi} \frac{\cosh(\beta)}{2 + 4\cosh(\beta)}. \tag{10}$$

We model the contribution of diffusion to the relaxation assuming complete depolarization of atoms on the cell walls. The density matrix is still described by a spin-temperature distribution, but the value of β now depends on the position in the cell. We find that for a wide range of conditions the contribution of diffusion to T_2 can be approximated with an accuracy of 30% by the classical solution for a freely decaying fundamental diffusion mode

$$\frac{1}{T_2^D} = qD\left(\frac{\pi}{a}\right)^2, \tag{11}$$

where a is the radius of the spherical cell. The relaxation rate is enhanced by the factor q because both electron and nuclear polarizations are destroyed at the walls.

Finally, we estimate the shot-noise limited sensitivity of the magnetometer based on the measured spin relaxation rates. The best sensitivity can be obtained using the optical rotation technique. The plane of polarization of the probe laser is modulated using a Faraday rotator with an amplitude α at a frequency ω_m (in our experiment $\omega_m = 3$ kHz and $\alpha = 2°$). The probe beam then passes through the cell and a linear polarizer set for maximum extinction. The transmitted signal is given by

$$I = I_0 \sin[\alpha \sin(\omega_m t) + \phi]^2. \tag{12}$$

A lock-in amplifier is used to detect the first harmonic proportional to the optical rotation angle ϕ introduced by the K vapor. Our calculations indicate that the optimal detuning of the probe laser is about 200 GHz and optimal probe laser intensity is 5 $\mathrm{mW/cm^2}$. We find that P_x polarization can be measured with a sensitivity of $2 \times 10^{-9}\ \mathrm{Hz^{-1/2}}$ and from Eq. (7) we obtain a shot-noise limited magnetic field sensitivity of $2 \times 10^{-18}\ \mathrm{T\,Hz^{-1/2}}$ in our 7 $\mathrm{cm^3}$ cell at 190 °C, with higher sensitivities possible at higher temperatures. This limit is far below the estimates of fundamental sensitivity limits for SQUID [21] or other alkali-metal magnetometers [3].

In conclusion, we have demonstrated a new type of alkali-metal magnetometer that is not affected by relaxation due to spin exchange. We obtained a magnetic field sensitivity of 10 $\mathrm{fT\,Hz^{-1/2}}$ limited only by thermal noise currents in our shields. Much higher sensitivity can be expected in a superconducting shield which does not have a thermal noise component. The magnetometer can be used in a wide range of applications. For example, a recently proposed technique to search for a permanent electron electric dipole moment [22] would directly benefit from a higher magnetic field sensitivity. While the dynamic range of the magnetometer is limited in the present implementation, it can be easily increased using a compensation coil and a suitable feedback system. By operating at higher temperatures, where K-K spin-destruction rate dominates the linewidth, one can increase the bandwidth of the magnetometer without sacrificing its sensitivity. For sufficiently high buffer gas pressures one can measure the magnetic fields independently in different parts of the cell by imaging the probe beam onto a multichannel photodetector. Such magnetic mapping capability would be useful for biomagnetic imaging. We thank Martin Boyd for constructing several components of the experiment. This work was supported by the University of Washington, a Precision Measurement Grant from NIST, NSF, NIH, and Princeton University.

*Author to whom correspondence should be addressed: romalis@princeton.edu

[1] E. B. Aleksandrov *et al.*, Opt. Sectrosc. **78**, 292 (1995).
[2] D. Budker, V. Yashchuk, and M. Zolotorev, Phys. Rev. Lett. **81**, 5788 (1998).
[3] D. Budker, D. F. Kimball, S. M. Rochester, V. V. Yashchuk, and M. Zolotorev, Phys. Rev. A **62**, 043403 (2000).
[4] S. Kadlecek, L. W. Anderson, and T. Walker, Nucl. Instrum. Methods Phys. Res., Sect. A **402**, 208 (1998).
[5] W. Happer and H. Tang, Phys. Rev. Lett. **31**, 273 (1973).
[6] S. Appelt *et al.*, Phys. Rev. A **58**, 1412 (1998).
[7] W. Happer and A. C. Tam, Phys. Rev. A **16**, 1877 (1977).
[8] T. G. Walker and W. Happer, Rev. Mod. Phys. **69**, 629 (1997).
[9] A. B. Baranga *et al.*, Phys. Rev. Lett. **80**, 2801 (1998).
[10] F. A. Franz and C. Volk, Phys. Rev. A **26**, 85 (1982).
[11] M. E. Wagshul and T. E. Chupp, Phys. Rev. A **49**, 3854 (1994).
[12] N. D. Bhaskar, J. Pietras, J. Camparo, W. Happer, and J. Liran, Phys. Rev. Lett. **44**, 930 (1980).
[13] N. Bevereni, P. Minguzzi, and F. Strumia, Phys. Rev. A **4**, 550 (1971).
[14] S. A. Murthy, D. Krause, Jr., Z. L. Li, and L. R. Hunter, Phys. Rev. Lett. **63**, 965 (1989).
[15] F. Grossette and J. Brossel, C.R. Acad. Sci. B **264**, 381 (1967).
[16] N. W. Ressler, R. H. Sands, and T. E. Stark, Phys. Rev. **184**, 102 (1969).
[17] T. Varpula and T. Poutanen, J. Appl. Phys. **55**, 4015 (1984).
[18] J. Nenonen and T. Katila, in *Proceedings of Biomagnetism '87*, edited by K. Atsumi *et al.* (Denki University Press, Tokyo, 1988), p. 426.
[19] J. Nenonen, J. Montonen, and T. Katila, Rev. Sci. Instrum. **67**, 2397 (1996).
[20] We neglect the effect of the nuclear magnetic moment of K atoms.
[21] Ya. S. Greenberg, Rev. Mod. Phys. **70**, 175 (1998).
[22] S. K. Lamoreaux, nucl-ex/0109014.